Spin-orbit strength driven crossover between intrinsic and extrinsic mechanisms of the anomalous Hall effect in epitaxial $L1_0$ FePd and FePt

K. M. Seemann,[1,*] Y. Mokrousov,[2] A. Aziz,[3] J. Miguel,[4] F. Kronast,[5] W. Kuch,[4]
M. G. Blamire,[3] A. T. Hindmarch,[1] B. J. Hickey,[1] I. Souza,[6] and C. H. Marrows[1,†]

[1]*School of Physics and Astronomy, University of Leeds, Leeds, LS2 9JT, United Kingdom*
[2]*Institut für Festkörperforschung and Institute for Advanced Simulation, Forschungszentrum Jülich, D-52425 Jülich, Germany*
[3]*Department of Materials Science and Metallurgy, University of Cambridge, Pembroke Street, Cambridge, CB2 3QZ, United Kingdom*
[4]*Freie Universität Berlin, Institut für Experimentalphysik, Arnimallee 14, D-14195 Berlin, Germany*
[5]*Helmholtz-Zentrum Berlin für Materialien und Energie, Albert-Einstein-Strasse 15, Berlin, Germany*
[6]*Department of Physics, University of California, Berkeley, CA 94720, USA*

(Dated: January 28, 2010)

We determine the composition of intrinsic as well as extrinsic contributions to the anomalous Hall effect (AHE) in the isoelectronic $L1_0$ FePd and FePt alloys. We show that the AHE signal in our 30 nm thick epitaxially deposited films of FePd is mainly due to extrinsic side-jump, while in the epitaxial FePt films of the same thickness and degree of order the intrinsic contribution is dominating over the extrinsic mechanisms of the AHE. We relate this crossover to the difference in spin-orbit strength of Pt and Pd atoms and suggest that this phenomenon can be used for tuning the origins of the AHE in complex alloys.

PACS numbers: 71.70.Ej, 75.50.Bb, 76.30.He

The anomalous Hall effect (AHE) in a ferromagnet as discovered by E. H. Hall in 1881 [1], can have its physical origin in bandstructure effects, i.e. be of intrinsic nature [2], or be driven by the scattering of the conduction electrons at magnetic impurities, which is called extrinsic AHE. The two basic extrinsic effects leading to AHE are the skew [3] and side-jump [4] scattering, and both are commonly understood to be a consequence of the spin-orbit interaction (SOI) acting on a conduction band electron. While many discoveries in the field of AHE are being made in both, experiments [5–7] but also computationally [8, 9], a joint effort is essential to explain the results of experiments with modern AHE theory. This becomes obvious when fitting the measured anomalous Hall resistivity ρ_{H} to the sum of linear and quadratic terms in diagonal resistivity ρ_0:

$$\rho_{\mathrm{H}} = \Phi_{\mathrm{Sk}}\rho_0 + \left(\kappa^{\mathrm{sj}} - \frac{e^2}{8\pi^3\hbar}\int_{\mathrm{BZ}}\Omega(\mathbf{k})d^3k\right)\rho_0^2. \qquad (1)$$

In this relation the linear term stands for skew-scattering [3], and the intrinsic contribution, given by an integral of the Berry curvature $\Omega(\mathbf{k})$ over pristine crystal's occupied electronic bands [10, 11], provides the Karplus-Luttinger part [2] of the anomalous Hall conductivity. Side-jump conductivity κ^{sj} accumulates all the other extrinsic contributions to ρ_{H}, quadratic in ρ_0 [4, 11]. Among the three contributions in Eq. (1), the intrinsic part can be calculated reasonably well from first-principles, while only model expressions for the extrinsic AHE exist up to now [11]. The ability to experimentally adjust the interplay between the different contributions of the AHE is of utter importance for the deeper understanding of this phenomenon, also with respect to developing a microscopic theory of extrinsic scattering mechanisms based on material's electronic structure. This may also be particularly valuable in prospect of novel applications at room temperature and above.

The epitaxially ordered ferromagnets $L1_0$-FePd and -FePt are ideal to evaluate the degree to which both extrinsic and intrinsic effects interplay in the experimentally observed AHE as they offer the possibility to controllably alter the strength of the SOI by exchanging isoelectronic atomic species Pd and Pt. Their well-defined crystal structure makes them amenable to theoretical analysis. Other physical phenomena such as domain wall resistance [12] of $L1_0$-ordered FePt and FePd have received in-depth investigation before [13–15]. Whilst there have been measurements of the AHE in these materials [16–19], a direct comparison between $L1_0$-ordered FePt and FePd with respect to AHE has not been carried out. In this Letter, the underlying physical effect of spin-orbit scattering in $L1_0$-ordered FePt and FePd is investigated, and we show in a combined experimental and theoretical study that whilst the AHE in FePd arises predominantly from extrinsic side-jump scattering, the much stronger SOI in FePt gives rise to a large intrinsic Berry phase AHE dominating over the side-jump contribution to the measured AHE signal.

Our experiments were performed on epitaxial thin films of $L1_0$-ordered FePd and FePt, which were deposited onto polished single crystalline MgO(100) substrates by dc magnetron co-sputtering as described in Ref. [15]. The epitaxial quality, i.e. the degree of chemical long range ordering S_{Order}, was determined by X-

TABLE I: Ordinary and anomalous Hall coefficients R_0 and $R_{\rm H}$ for the L1$_0$-ordered FePt and FePd epilayers at $T = 50$ and 270 K.

	R_0 (50 K) nΩcm/T	R_0 (270 K) nΩcm/T	$R_{\rm H}$ (50 K) $\mu\Omega$cm/T	$R_{\rm H}$ (270 K) $\mu\Omega$cm/T
FePd	-28 ± 3	-16 ± 2	0.01 ± 0.01	0.14 ± 0.05
FePt	-3 ± 1	-2 ± 1	0.12 ± 0.05	0.75 ± 0.10

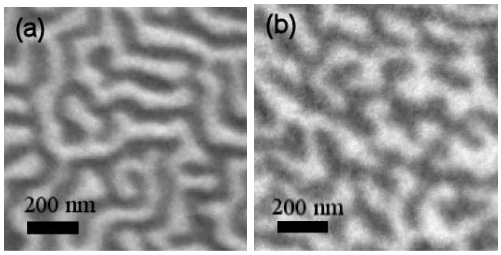

FIG. 1: XMCD-PEEM images of 1 μm $\times$ 1 μm area of the room temperature demagnetized domain state of (a) L1$_0$-ordered FePd and (b) FePt films in zero magnetic field. Dark and bright areas depict magnetic domains of oppositely orientated magnetization perpendicular to the film plane.

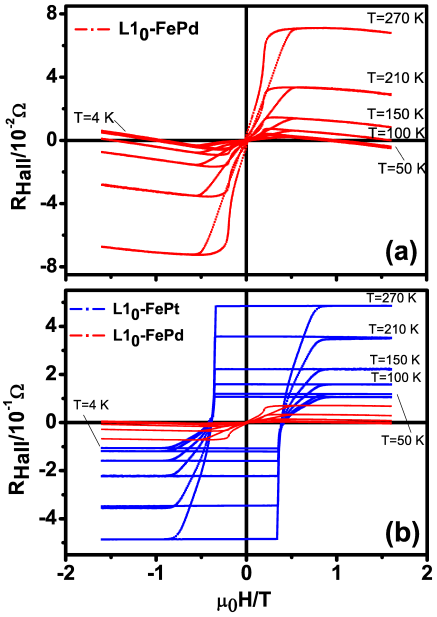

FIG. 2: (Color online) Measured Hall resistance $R_{\rm Hall}$ for various temperatures ranging between $T = 4$ K to 270 K for (a) L1$_0$-FePd and (b) L1$_0$-FePt epilayers. The measured AHE signal is, for all temperatures, much larger in L1$_0$-FePt as compared to L1$_0$-FePd, as shown in (b).

ray diffraction, whilst the nominal film thicknesses were confirmed by X-ray reflectometry. We have deliberately selected films of comparable thickness t of 31 ± 1 nm (FePd) and 34 ± 1 nm (FePt), and degree of chemical ordering $S_{\rm Order} = 0.8 \pm 0.1$ to be able to compare the magnetotransport properties as closely as possible.

The highly anisotropic L1$_0$-crystal lattice and strong SOI from the 4d and 5d species give rise to a very strong magnetocrystalline anisotropy with a uniaxial easy axis normal to the film plane. This yields a dense labyrinth domain pattern after ac demagnetization. We imaged this zero-field domain state in both films by means of X-ray magnetic circular dichroism-photoelectron emission microscopy (XMCD-PEEM) [20] at the UE49-PGM-a microfocus beamline of the BESSY II facility. We used the XMCD effect at the Fe L_3-absorption edge at 707 eV to image the magnetic domains of the FePt and FePd thin films, and the resulting images are shown in Fig. 1. The images are represented as greyscale coded absorption asymmetry for opposite helicities of the circularly polarized X-rays, $A_{\rm PEEM} = \frac{I_+ - I_-}{I_+ + I_-}$. For constant absolute value of the magnetic moments, $A_{\rm PEEM}$ is proportional to the projection of the local magnetization on the direction of incidence of the light.

Both domain patterns show the characteristic maze structure obtained at zero-field for the L1$_0$-ordered Fe-alloys investigated [15, 17]. From the 1×1 μm^2 area PEEM images we determine the average domain width of $\overline{D}_{\rm PEEM} = 69 \pm 20$ nm for FePd and $\overline{D}_{\rm PEEM} = 125 \pm 30$ nm for FePt, typical values for films of this thickness and degree of crystallographic order[14, 15, 21]. High crystallographic long range order parameter of $S_{\rm Order} \approx 0.8$ determined from X-ray diffractometry together with the experimental verification by XMCD-PEEM of the demagnetized domain state simulated from measured micromagnetic parameters serve as evidence for the L1$_0$-phase of our samples.

The typical hysteretic property of the Hall resistance $R_{\rm Hall}$ is obtained from 4-probe dc Hall measurements and shown in Fig. 2(a) and (b) for both L1$_0$-ordered FePd and FePt. Describing the total Hall resistivity as $\rho_{\rm Hall} = R_0 H + R_{\rm H} M$, with R_0 and $R_{\rm H}$ the ordinary and anomalous Hall coefficients, we find a weak ordinary Hall resistance in FePd (Fig. 2(a)), noticeable in the shallow slope of the saturation regions of the Hall loop. The ordinary Hall coefficient R_0 in the FePt sample is at least an order of magnitude lower than in FePd at all temperatures, and can safely be considered negligible in comparison to the anomalous Hall signal itself, in this material being an order of magnitude larger than in FePd (see also Table I). The evolution of both the anomalous Hall resistivity $\rho_{\rm H}$ and the longitudinal resistivity ρ_0 with temperature was determined by extrapolating from the magnetically saturated state back to zero field for each value of T. The negative sign of R_0 is the same for both materials, as is the positive sign of the AHE coefficient $R_{\rm H}$. Negative ordinary Hall coefficients correspond to electron-like transport. The ordinary and anomalous Hall coefficients are shown for two different temperatures in Table I.

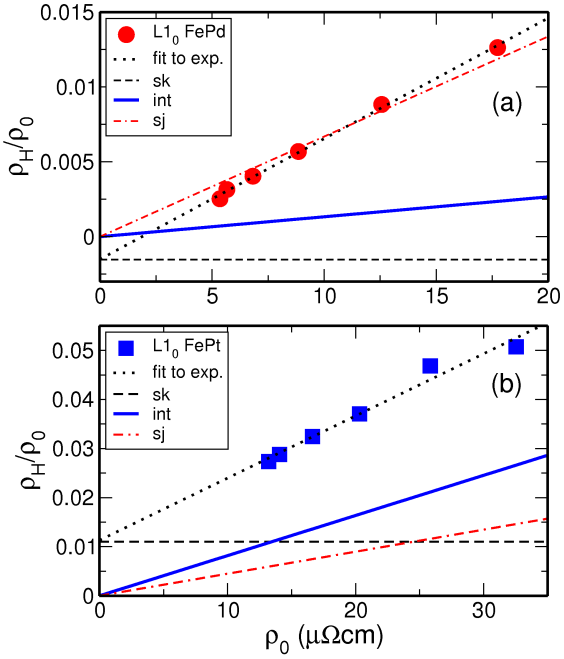

FIG. 3: (Color online) Resistivity ratio of measured transverse and longitudinal resistivity ρ_H/ρ_0 vs. longitudinal resistivity ρ_0 for (a) L1$_0$-FePd (circles) and (b) L1$_0$-FePt (squares). The thin black dotted line is a linear $\Phi_{Sk}+\kappa\rho_0$ fit to the measured ratio yielding Φ_{Sk} (dashed line) and κ. The intrinsic contribution $\kappa^{int}\rho_0$ (solid thick line) calculated from first principles as well as the side-jump contribution $(\kappa-\kappa^{int})\rho_0 = \kappa^{sj}\rho_0$ (dot-dashed line) yield a linear dependence in ρ_H/ρ_0 vs. ρ_0 (see also Table II). The total ρ_H/ρ_0 signal is a sum of skew-scattering Φ_{Sk}, intrinsic and side-jump contributions.

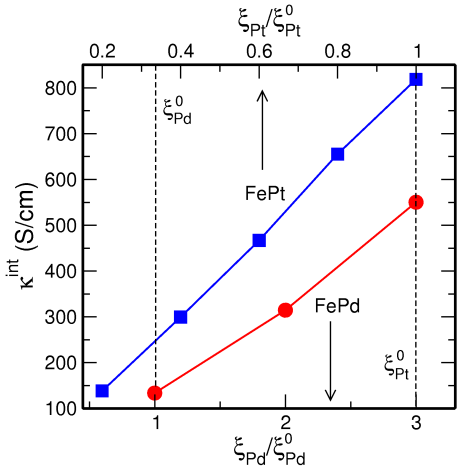

FIG. 4: (Color online) Dependence of the *ab initio* calculated intrinsic anomalous Hall conductivity κ^{int} on the strength of the spin-orbit interaction inside the Pd atoms in $L1_0$-FePd, ξ_{Pd} (circles) and Pt atoms in $L1_0$-FePt, ξ_{Pt} (squares), with respect to their unscaled values $\xi^0_{Pd} = 0.19$ eV and $\xi^0_{Pt} = 0.54$ eV (dashed lines).

In order to distinguish the various contributions to the experimental AHE transport data we relate ρ_H to the longitudinal resistivity ρ_0 employing a $\rho_H = \Phi_{Sk}\rho_0 + \kappa\rho_0^2$ fit to experimental data for the two compounds [11]. We assume that Φ_{Sk} and κ are constant and do not depend on temperature T via temperature-dependent magnetization [22], as the measurements are performed at T well below T_C. According to Eq. (1), parameter κ stands for the anomalous Hall conductivity and incorporates the intrinsic and side-jump channels for the AHE, while Φ_{Sk} is the skew-scattering angle [23]. In Fig. 3 we present the experimental ρ_H/ρ_0 ratio plotted versus ρ_0, and its linear $\Phi_{Sk}+\kappa\rho_0$ fit for FePd and FePt. This fit yields values for κ in FePd and FePt of 806 S/cm and 1267 S/cm, respectively. The extracted values of the skew-scattering angle Φ_{Sk} for the two compounds, given as an offset along the y-axis in Fig. 3, are opposite in sign, with Φ_{Sk} of -1.5 mrad in FePd much smaller than that of $+11.0$ mrad in FePt (see Table II). However, in our AHE experiments the ρ_H resistivity is measured *in summa*, i.e. its value remains positive for the whole range of measured ρ_0.

In order to assess the intrinsic part of the AHE, we performed *ab initio* calculations for both materials, L1$_0$-FePd and L1$_0$-FePt, in both cases for the perfectly ordered (S_{Order}=1) systems, using the full-potential linearized augmented plane-wave (FLAPW) method as implemented in the Jülich density functional theory code FLEUR [24] and using the Wannier interpolation procedure of Wang *et al.* [25] for the Brillouin zone integration of the Berry curvature [26]. Our calculated values of the intrinsic anomalous Hall conductivity, κ^{int}, are given in Table II and constitute 818 S/cm for FePt and 133 S/cm for FePd. While in FePt the value of κ^{int} accounts for 65% of experimentally measured κ, in FePd the intrinsic contribution constitutes only 15% of the experimentally measured conductivity. This strongly suggests that if in FePt the intrinsic mechanism is the dominant source of κ, in isoelectronic FePd it is extrinsic side-jump scattering which provides a major contribution to it. Estimating the side-jump contribution to the conductivity κ^{sj} as the difference between the measured κ and the calculated κ^{int}, we observe a clear crossover between the two contributions to the conductivity κ with κ^{int}(FePt) $>$ κ^{sj}(FePt) and κ^{int}(FePd) $\ll$ κ^{sj}(FePd), Table II. Overall, by comparing the intrinsic, side-jump and skew-scattering contributions to the total measured ρ_H/ρ_0 ratio, presented in Fig. 3, we observe that while in FePd the measured ρ_H resistivity is mainly due to side-jump, the AHE signal in FePt samples presents a competition between dominant intrinsic and extrinsic channels of the AHE.

The crossover between the intrinsic-dominated AHE in FePt and the side-jump domaninated effect in FePd is caused mainly by the different spin-orbit coupling strengths in the two materials. We show this by artificially scaling the spin-orbit strength ξ inside the Pt and Pd atoms, which is determined as an average of SOI

TABLE II: Coefficients of the linear $\Phi_{\rm Sk} + \kappa\rho_0$ fit to the experimental ρ_H/ρ_0 ratio for FePd and FePt (Fig. 2), the skew scattering angle $\Phi_{\rm Sk}$ and conductivity κ. $\kappa^{\rm int}$ stands for the calculated from *ab initio* value of the intrinsic conductivity, while the side-jump conductivity $\kappa^{\rm sj}$ is obtained as $\kappa - \kappa^{\rm int}$.

	$\Phi_{\rm Sk}$	κ	$\kappa^{\rm int}$	$\kappa^{\rm sj}$
	mrad	S/cm	S/cm	S/cm
FePd	-1.5 ± 0.2	806 ± 18	133	669
FePt	$+11.0 \pm 2$	1267 ± 101	818	449

matrix elements calculated on corresponding d-orbitals. Figure 4 shows the calculated intrinsic anomalous Hall conductivity (AHC) of FePd as the SOI strength $\xi_{\rm Pd}$ inside the Pd atoms is artificially increased three-fold until it reaches the actual value in the Pt atoms. It is seen that the intrinsic AHC in FePd increases from 133 S/cm to 550 S/cm, which is comparable to the value of 818 S/cm calculated in FePt. Conversely, upon decreasing the SOI strength in the Pt atoms by a factor of three, the AHC of FePt decreases to about 250 S/cm. The remaining differences between the intrinsic AHC in FePt and FePd can be accounted for by their different lattice constants, orbitals spreads, and Stoner parameters.

On the other hand, according to Table II, while $\kappa^{\rm int}$ increases the side-jump conductivity $\kappa^{\rm sj}$ decreases moderately with increasing SOI strength. Such behavior can be seen from model calculations for a 2D model Hamiltonian, namely, massive Dirac Hamiltonian with randomly distributed weak δ-function-like spin-independent impurities [27]. In this case the ratio of the intrinsic and side-jump conductivities can be deduced analytically and constitutes $\kappa^{\rm int}/\kappa^{\rm sj} = \xi^2 + 1/4$, where $\xi = \Delta/(vk_F)$ is the scaled SOI strength Δ, v is the parameter of the model, and k_F is the Fermi wave vector determined by the band filling [27]. It is clear that, while for large SOI the intrinsic κ dominates over $\kappa^{\rm sj}$, for comparatively small ξ the side-jump can be several times larger than $\kappa^{\rm int}$ within this model [28]. In our work, we provide the first experimental verification of this phenomenon in a bulk material with a complex electronic structure. Moreover, we suggest that this phenomenon may be employed to adjust the ratio of intrinsic and extrinsic contributions to the AHE with the prospect of engineering materials with desired AHE properties. For example maximizing AHE in the $FePt_xPd_{1-x}$ $L1_0$ alloys [29] by adjusting the ratio between side-jump and intrinsic AHE and tuning the skew-scattering by impurity concentration at the same time may lead to novel devices.

The authors thank G. Obermeier, J. Cunningham, M.C. Hickey, A. Blackburn for fruitful discussions and P. Cale, G. Butterworth and T. Haynes for technical assistance. Financial support by the UK EPSRC (Spin@RT), by the BMBF (05KS4UK1/4) and the DFG (project MO 1731/1-1) is gratefully acknowledged.

* Present address: Institut für Festkörperforschung (IFF-9), FZ Jülich GmbH, D-52425 Jülich, Germany; Electronic address: k.seemann@fz-juelich.de
† Electronic address: c.h.marrows@leeds.ac.uk

[1] E. H. Hall, Philos. Mag. **12**, 157 (1881).
[2] R. Karplus and J. M. Luttinger, Phys. Rev. **95**, 1154 (1954).
[3] J. Smit, Physica (Amsterdam) **24**, 39 (1958).
[4] L. Berger, Phys. Rev. B **2**, 4559 (1970).
[5] W. R. Branford, K. A. Yates, E. Barkhoudarov, et al., Phys. Rev. Lett. **102**, 227201 (2009).
[6] K. S. Takahashi, M. Onoda, M. Kawasaki, et al., Phys. Rev. Lett. **103**, 057204 (2009).
[7] Y. Tian, L. Ye, and X. Jin, Phys. Rev. Lett. **103**, 087206 (2009).
[8] Y. Yao, L. Kleinman, A. H. MacDonald, et al., Phys. Rev. Lett. **92**, 037204 (2004).
[9] E. Roman, Y. Mokrousov, and I. Souza, Phys. Rev. Lett. **103**, 097203 (2009).
[10] M. V. Berry, Proc. R. Soc. Lond. A **392**, 45 (1984).
[11] N. Nagaosa, J. Sinova, S. Onoda, et al., Rev. Mod. Phys., accepted (2009).
[12] C. H. Marrows, Adv. Phys. **54**, 585 (2005).
[13] D. Ravelosona, A. Cebollada, F. Briones, et al., Phys. Rev. B **59**, 4322 (1999).
[14] C. H. Marrows and B. C. Dalton, Phys. Rev. Lett. **92**, 097206 (2004).
[15] K. M. Seemann, V. Baltz, M. MacKenzie, et al., Phys. Rev. B **76**, 174435 (2007).
[16] M. Viret, Y. Samson, P. Warin, et al., Phys. Rev. Lett. **85**, 3962 (2000).
[17] J. Yu, U. Rüdiger, A. D. Kent, et al., J. Appl. Phys. **87**, 6854 (2000).
[18] A. P. Mihai, J. P. Attané, A. Marty, et al., Phys. Rev. B **77**, 060401(R) (2008).
[19] J. Moritz, B. Rodmacq, S. Auffret, et al., J. Phys. D: Appl. Phys. **41**, 135001 (2008).
[20] J. Stöhr, Y. Wu, B. D. Hermsmeier, et al., Science **259**, 658 (1993).
[21] K. M. Seemann, M. C. Hickey, V. Baltz, et al., unpublished.
[22] C. Zheng, Y. Yao, Q. Niu, et al., Phys. Rev. Lett. **96**, 037204 (2006).
[23] We also applied to our data the alternative fit from Ref. [7]. We find that it yields similar values for the impurity-related skew scattering as the current fit, and leads to the same crossover behavior between the intrinsic and side-jump contributions to the AHE in both alloys.
[24] URL `http://www.flapw.de`.
[25] X. Wang, J. R. Yates, I. Souza, et al., Phys. Rev. B **74**, 195118 (2006).
[26] For computational details see "Supplementary material".
[27] N. A. Sinitsyn, A. H. MacDonald, T. Jungwirth, et al., Phys. Rev. B **75**, 045315 (2007).
[28] For evaluating the $\kappa^{\rm int}/\kappa^{\rm sj}$ ratio we assume that $\kappa^{\rm sj}$ accumulates both side-jump and anomalous distribution contributions [27], indistinguishable experimentally, while we neglect the intrinsic skew-scattering.
[29] S. D. Willoughby, J. M. MacLaren, T. Ohkubo, et al., J. Appl. Phys. **91**, 8822 (2002).